ELSEVIER

Journal of Organometallic Chemistry 637–639 (2001) 521–530

Journal of Organometallic Chemistry

www.elsevier.com/locate/jorganchem

Synthesis, reactivity, and crystal structures of ferrocene-substituted amidinate derivatives

John R. Hagadorn [1], John Arnold *

Department of Chemistry, University of California, 526 Latimer Hall, Berkeley, CA 94720-1460, USA

Received 19 April 2001; received in revised form 15 May 2001; accepted 17 May 2001

Abstract

Reaction of FcLi (Fc = ferrocenyl) with DCC (DCC = 1,3-dicyclohexylcarbodiimide), followed by the addition of water, yields the ferrocene-containing amidine Fc(NCy)NHCy in 50% yield. The amidine is readily deprotonated by $LiN(SiMe_3)_2$ or $NaN(SiMe_3)_2$ to yield alkali metal amidinates, $[FcC(NCy)_2]Li$ and $[FcC(NCy)_2]Na$, in high yields. These serve as convenient sources of $[FcC(NCy)_2]^-$ for a wide range of salt-metathesis reactions with transition metal halides. Reactions of $[FcC(NCy)_2]Li$ with 0.5 equivalents MX_2 (M = Fe, Co; X = Cl, Br) form the paramagnetic 4-coordinate derivatives $[FcC(NCy)_2]_2M$. Reaction of $[FcC(NCy)_2]Na$ with $CpFe(CO)_2I$ affords the carbamoyl derivative CpFe(CO)[FcC(NCy)N(Cy)C(O)]. Although not thermally labile, a CO ligand is readily lost upon UV irradiation to give the amidinate derivative $CpFe(CO)[FcC(NCy)_2]$. The addition of ^{13}CO (50 psig) to a solution of $CpFe(CO)[FcC(NCy)_2]$ results in the rapid exchange of CO at 25 °C. Heating this solution to 80 °C results in the partial formation of the carbamoyl species by a formal CO insertion into an Fe–N bond. Reaction of $[FcC(NCy)_2]Li$ with 0.5 equivalents $[Rh(CO)_2(\mu\text{-}Cl)]_2$ forms orange $[FcC(NCy)_2]Rh(CO)_2$ in good yield. Cyclic voltammetry measurements in THF reveal a quasi-reversible oxidation at $E_{1/2} = +0.46$ V followed by an irreversible oxidation at +1.49 V (vs. Cp_2Fe). Chemical oxidation of $[FcC(NCy)_2]Rh(CO)_2$ with $AgBF_4$ generates the amidine-containing product $\{[FcC(NCy)NHCy]Rh(CO)_2\}[BF_4]$.

Keywords: Amidinates; Ferrocene ligands; Cobalt; Iron; Rhodium

1. Introduction

Transition metal amidinate complexes have been attracting significant interest for over 20 years due to their diverse structural and reaction chemistry [1]. Notably, they have been used for the preparation of metal–metal bonded species [2], dinitrogen complexes [2a,3], and catalysts for a wide range of bond forming reactions (C–C and C–N) [4], including olefin polymerizations [5]. With the current interest in organometallic chemistry of controlling structure/reactivity through ligand modification, a wide range of new amidinates has been reported in the last several years. These include typical $[RC(NR')_2]^-$ amidinates [6], tethered bis(amidinates) [7], chiral versions [5c,7], and amidinates with pendant donors [8]. Toward this end, we recently reported the first Fc-substituted (Fc = ferrocenyl) amidinate, which by virtue of the redox-active Fc-unit, has potential in a wide range of applications such as metal-containing polymers, polymetallic complexes, and electrochemically controlled ('redox switched') catalysts [9]. Here, we give a detailed report of the synthesis and characterization of several new Fe(II) and Rh(I) derivatives of the Fc-containing amidinate ligand.

2. Experimental

2.1. General considerations

Standard Schlenk-line and glove box techniques were used throughout the preparative procedures except in the work-up of air-stable FcC(NCy)NHCy (Cy = cyclohexyl, Fc = ferrocenyl). Ferrocene, $AgBF_4$, and *t*-BuLi were purchased from Strem and used as received. 1,3-

* Corresponding author. Fax: +1-508-437-7852.
E-mail address: arnold@socrates.berkeley.edu (J. Arnold).
[1] Current Address: Department of Chemistry and Biochemistry, University of Colorado, Boulder, CO 80309-0215, USA.

0022-328X/01/$ - see front matter
PII: S0022-328X(01)00973-1

Dicyclohexylcarbodiimide (DCC) was purchased from Sigma and used as received. $FeCl_2$ and $CoBr_2$ were purchased from Strem and dried at 150 °C/10^{-2} mmHg overnight. $LiN(SiMe_3)_2$ [10], $NaN(SiMe_3)_2$ [11], $[Rh(CO)_2(\mu\text{-}Cl)]_2$ [12], and $CpFe(CO)_2I$ [13] were prepared following literature procedures. Tetrahydrofuran (THF), Et_2O, and hexanes were distilled from sodium/benzophenone under nitrogen. Toluene was distilled from sodium under nitrogen. CH_2Cl_2 was distilled from CaH_2 under nitrogen. C_6D_6 was vacuum transferred from sodium/benzophenone. $CDCl_3$ was vacuum transferred from CaH_2. Melting points were determined in sealed capillary tubes under nitrogen and are uncorrected. ^{1}H- and $^{13}C\{^1H\}$-NMR spectra were recorded at ambient temperatures unless stated otherwise. Chemical shifts (δ) are given relative to residual protium in the deuterated solvent at 7.15 and 7.24 ppm for C_6D_6 and $CDCl_3$, respectively. IR samples were prepared as mineral oil mulls and taken between KBr plates. Elemental analyses were determined within the College of Chemistry, University of California, Berkeley. Cyclic voltammetry measurements were conducted with 10^{-2} M solutions (in CH_2Cl_2 or THF) using 0.1 M $[Bu_4N]PF_6$ as the supporting electrolyte. The salt was purified by recrystallization prior to use [14]. A standard three-electrode assembly consisting of a platinum working, platinum auxiliary, and a silver reference was used for the measurements. Magnetic moments were determined using Evans' method [15]. Single crystal X-ray structure determinations were performed at CHEXRAY, University of California, Berkeley.

2.2. Syntheses

2.2.1. FcC(NCy)NHCy

Ferrocene (100 g, 538 mmol) was evacuated for 2 h in a 2-l round-bottomed flask. Tetrahydrofuran (300 ml) and hexanes (300 ml) were added forming an orange suspension. At 0 °C, a pentane solution of *t*-BuLi (328 ml, 538 mmol) was added dropwise over 1.5 h. The reaction mixture was allowed to warm to ambient temperature over 2 h. After stirring overnight, a THF (100 ml) solution of DCC (111 g, 538 mmol) was added dropwise over 30 min. After stirring the orange suspension overnight, degassed H_2O (19.4 ml, 1080 mmol) was added dropwise forming a dark orange solution and a white solid. The orange solution was decanted, and the volatile materials were removed using a rotary evaporator. The resulting orange solid was sublimed overnight at 65 °C/10^{-2} mmHg to remove unreacted Cp_2Fe and DCC. The remaining solid was crystallized from boiling hexanes to yield orange prisms of the product. Two crops: 106 g, 50% yield. M.p.: 109.5–111.0 °C. ^{1}H-NMR (C_6D_6): $\delta = 4.63$ (d, $J = 6.8$ Hz, 1H, NH), 4.28 (t, $J = 1.8$ Hz, 2H, α-C_5H_4), 4.18 (m, 1H, Cy), 3.99 (s, 5H, C_5H_5), 3.93 (t, $J = 1.8$ Hz, 2H, β-C_5H_4), 3.55 (m, 1H, Cy), 2.21 (m, 2H, Cy), 1.80–1.10 (m, 18H, Cy). $^{13}C\{^1H\}$-NMR (C_6D_6): $\delta = 151.3$, 81.4, 69.5, 69.4, 68.2, 58.3, 48.9, 36.5, 33.7, 26.5, 25.3. IR (cm^{-1}): 3420 (m, ν_{N-H}), 1619 (vs, $\nu_{C=N}$), 1490 (s), 1301 (w), 1256 (w), 1181 (w), 1156 (w), 1106 (w), 1023 (w), 1003 (w), 888 (w), 830 (m), 722 (w), 568 (w), 488 (w). Anal. Found: C, 70.41; H, 8.46; N, 7.05. Calc. for $C_{23}H_{32}N_2Fe$: C, 70.41; H, 8.22; N, 7.14%.

2.2.2. {[FcC(NCy)$_2$]Li(Et$_2$O)}$_2$

Toluene (200 ml) cooled to −78 °C was added to FcC(NCy)NHCy (17.1 g, 43.6 mmol) and $LiN(SiMe_3)_2$ (7.30 g, 43.6 mmol) forming a clear orange solution. After stirring overnight at room temperature (r.t.), the solution was concentrated to a viscous dark orange solution. Addition of Et_2O (100 ml) followed by cooling to −40 °C yielded the product as orange crystals (13.4 g). A second crop yielded additional crystals (4.9 g). Total yield: 89%. M.p.: 225–230 °C. ^{1}H-NMR (C_6D_6): $\delta = 5.0$–4.1 (br, 9H, C_5H_5, C_5H_4), 3.26 (q, 4H, Et_2O), 2.6–1.2 (br, 22H, Cy), 1.11 (t, 6H, Et_2O). IR (cm^{-1}): 1492 (s), 1342 (m), 1305 (w), 1153 (w), 1106 (w), 1064 (w), 1024 (w), 1002 (w), 982 (w), 888 (w), 818 (m), 742 (w), 722 (w), 498 (w), 473 (w). Anal. Found: C, 68.89; H, 8.62; N, 5.82. Calc. for $C_{27}H_{41}N_2FeLiO$: C, 68.65; H, 8.75; N, 5.93%.

2.2.3. [FcC(NCy)$_2$]$_2$Fe(Et$_2$O)$_{0.25}$

Tetrahydrofuran (30 ml) was added to a 100-ml round-bottomed flask containing $FeCl_2$ (0.135 g, 1.06 mmol) and $[FcC(NCy)_2]Li(Et_2O)$ (1.00 g, 2.13 mmol) to form an orange–brown solution. After stirring overnight, the volatile materials were removed under reduced pressure. The orange solid was extracted with CH_2Cl_2 (25 ml) and filtered through a Celite pad on a fritted disk. Concentration to saturation, followed by the addition of Et_2O (20 ml) and cooling to −40 °C afforded the product as orange crystals (0.55 g, 61%). M.p.: 216–218 °C. IR (cm^{-1}): 1451 (vs, br), 1376 (m), 1306 (w), 1232 (w), 1204 (w), 1054 (s, br), 901 (m), 824 (m), 722 (m), 562 (m), 533 (w), 522 (w), 497 (m), 479 (m). Anal. Found: C, 65.69; H, 7.52; N, 6.48. Calc. for $C_{47}H_{64.5}Fe_3N_4O_{0.25}$: C, 65.86; H, 7.58; N, 6.54%. $\mu_{eff} = 5.02\ \mu_B$.

2.2.4. [FcC(NCy)$_2$]$_2$Co(Et$_2$O)

Ethyl ether (100 ml) was added to a 250-ml round-bottomed flask containing $CoBr_2$ (1.00 g, 4.57 mmol) and $[FcC(NCy)_2]Li(Et_2O)$ (4.30 g, 9.14 mmol) to form a brown suspension. After stirring overnight, the volatile materials were removed under reduced pressure, and the brown solid was extracted with toluene (60 ml). The solution was filtered through a Celite pad on a fritted disk and concentrated to 20 ml. The addition of hexanes (20 ml) and cooling to −40 °C afforded an ochre solid (2.85 g, 74%). Recrystallization from Et_2O gave

analytically pure product co-crystallized with solvent. M.p.: 203–207 °C. IR (cm^{-1}): 1631 (w), 1451 (vs, br), 1376 (m), 1364 (m), 1308 (w), 1236 (w), 1204 (w), 1159 (w), 1120 (w), 1108 (w), 1076 (w), 1030 (w), 1002 (w), 990 (w), 902 (m), 824 (m), 572 (m), 497 (w), 479 (w). Anal. Found: C, 65.42; H, 7.55; N, 6.29. Calc. for $C_{50}H_{72}COFe_2N_4O$: C, 65.58; H, 7.92; N, 6.12%. $\mu_{eff} = 4.62\ \mu_B$.

2.2.5. Preparation of [FcC(NCy)$_2$]Na

Hexanes (200 ml) were added to FcC(NCy)NHCy (22.0 g, 56.2 mmol) and $NaN(SiMe_3)_2$ (10.3 g, 56.2 mmol) forming an orange suspension. After stirring overnight, the orange solid was collected by filtration and dried under reduced pressure affording an orange powder (22.6 g, 97.0%).

2.2.6. CpFe(CO)[FcC(NCy)N(Cy)C(O)]

Toluene (100 ml) was added to $CpFe(CO)_2I$ (2.32 g, 7.65 mmol) and [FcC(NCy)$_2$]Na (3.17 g, 7.65 mmol) to form a black solution. After a few minutes, the solution became orange–brown with the formation of a yellow precipitate. The solution was stirred overnight and then filtered through a pad of Celite on a fritted disk. Concentration to 20 ml and cooling to −40 °C yielded the product as an orange solid (1.00 g). The addition of hexanes (20 ml) to the mother liquor followed by cooling to −40 °C yielded a second crop as orange–red crystals. Total yield 2.50 g, 57.5%. M.p.: 194–195 °C. ^{1}H-NMR (C_6D_6): $\delta = 4.69$ (m, 1H, α-C_5H_4), 4.54 (s, 5H, C_5H_5), 4.18 (m, 1H, α-C_5H_4), 3.96 (s, 5H, C_5H_5), 3.96 (m, 1H, β-C_5H_4), 3.93 (m, 1H, β-C_5H_4), 3.56 (m, 1H, Cy), 3.04 (m, 2H, Cy), 2.33 (m, 1H, Cy), 1.8–0.9 (m, 17H, Cy). ^{13}C{^{1}H}-NMR (C_6D_6): $\delta =$ 233.8, 220.3, 166.0, 84.1, 76.2, 71.6, 70.2, 70.0, 69.3, 68.1, 62.4, 60.4, 37.6, 35.4, 32.6, 31.3, 27.3, 27.2, 25.9, 25.8, 25.7, 25.7. IR (cm^{-1}): 1902 (vs, ν_{CO}), 1630 (s, $\nu_{C=O}$), 1514 (m, $\nu_{C=N}$), 1459 (s, br), 1377 (s), 1212 (m), 1157 (w), 1118 (w), l061 (w), 998 (w), 964 (w), 924 (w), 876 (w), 829 (w), 814 (w), 795 (w), 727 (w), 666 (w), 570 (w), 496 (w), 474 (w). Anal. Found: C, 64.00; H, 6.57; N, 4.91. Calc. for $C_{30}H_{36}Fe_2N_2O_2$: C, 63.40; H, 6.38; N, 4.93%.

2.2.7. CpFe(CO)[FcC(NCy)$_2$]

Toluene (200 ml) was added to $CpFe(CO)_2I$ (10.0 g, 32.9 mmol) and [FcC(NCy)$_2$]Na (13.6 g, 32.9 mmol) forming a black solution. After a few minutes, the solution became orange–brown with the formation of a yellow precipitate. The solution was stirred overnight and then filtered through a pad of Celite on a fritted disk into a long quartz tube (ca. 2.5 cm diameter). The solution was irradiated in an UV chamber for 24 h under N_2. ^{1}H-NMR spectroscopic analysis of an aliquot of the solution confirmed the absence of starting material. The solution was filtered and concentrated to 50 ml. The addition of hexanes (100 ml) and cooling to −40 °C yielded the product as dark red crystals (3.5 g). A second crop was obtained by concentration and cooling to −40 °C. Total yield: 4.65 g, 26.5%. M.p.: 176–185 °C. ^{1}H-NMR (C_6D_6): $\delta = 4.43$ (s, 5H, C_5H_5), 4.04–4.02 (m, 7H, C_5H_5 + α-C_5H_4), 3.87 (t, $J = 1.7$ Hz, 2H, β-C_5H_4), 3.60 (m, 2H, Cy), 1.9–1.0 (m, 20H, Cy). ^{13}C{^{1}H}-NMR (C_6D_6): $\delta = 223.2$, 166.1, 79.3, 74.9, 69.8, 69.1, 68.0, 55.5, 38.2, 36.5, 26.3, 26.2. IR (cm^{-1}): 1922 (vs, ν_{CO}), 1523 (m), 1465 (vs, br), 1377 (s), 1307 (w), 1231 (w), 1122 (w), 1106 (w), 1089 (w), 1056 (w), 1001 (w), 900 (w), 836 (w), 823 (w), 808 (w), 722 (w), 559 (w), 528 (w), 502 (w), 482 (w). Anal. Found: C, 64.30; H, 6.83; N, 4.85. Calc. for $C_{29}H_{36}Fe_2N_2O$: C, 64.47; H, 6.72; N, 5.18%.

2.2.8. [FcC(NCy)$_2$]Rh(CO)$_2$

Toluene (35 ml) was added to $[Rh(CO)_2(\mu\text{-}Cl)]_2$ (0.337 g, 0.867 mmol) and [FcC(NCy)$_2$]Li(Et$_2$O) (0.816 g, 1.73 mmol) forming a cloudy, orange–brown solution. After stirring for 5 h, the volatile materials were removed under reduced pressure. The orange–brown solid was extracted with hexanes (80 ml) and filtered through a pad of Celite on a fritted disk. Concentration of the solution to 60 ml and cooling to −40 °C afforded the product as orange crystals (0.52 g). Total yield from two crops: 0.78 g, 82%. M.p.: 134–136 °C. ^{1}H-NMR (C_6D_6): $\delta = 4.15$ (t, $J = 1.9$ Hz, 2H, α-C_5H_4), 3.97 (s, 5H, C_5H_5), 3.96 (t, $J = 1.9$ Hz, 2H, β-C_5H_4), 3.84 (m, 2H, Cy), 1.67 (m, 8 H, Cy), 1.48 (m, 2H, Cy), 1.4–1.0 (m, 10H, Cy). ^{13}C{^{1}H}-NMR (C_6D_6): $\delta = 188.4$ (d, $^1J_{Rh-C} = 67.1$ Hz), 182.3 ($^2J_{Rh-C} = 4.4$ Hz), 72.7, 70.0, 70.0, 69.2, 54.4, 37.0, 26.0, 25.8. IR (cm^{-1}): 2052 (vs), 1977 (vs), 1511 (m), 1462 (m), 1451 (s), 1377 (m), 1361 (m), 1237 (m), 1123 (w), 1107 (w), 1080 (w), 1029 (w), 1004 (w), 821 (m), 569 (m), 519 (m), 475 (m). Anal. Found: C, 54.50; H, 5.65; N, 5.09. Calc. for $C_{25}H_{31}FeN_2O_2Rh$: C, 54.57; H, 5.68; N, 5.09%.

2.2.9. {[FcC(NCy)NHCy]Rh(CO)$_2$}[BF$_4$]

Methylene chloride (20 ml) was added to powdered [FcC(NCy)$_2$]Rh(CO)$_2$ (0.152 g, 0.276 mmol) and $AgBF_4$ (54.8 mg, 0.282 mmol) to form a burgundy-colored solution. Within a few minutes a silver precipitate was observed. After 3 h, the volatile materials were removed under reduced pressure. The red–violet residue was extracted with CH_2Cl_2 (20 ml) and filtered. The solution was concentrated to 7 ml and cooled to −40 °C. After sitting overnight, the solution was filtered again to remove some silver-colored precipitate, and Et_2O (10 ml) was added. Within a few hours, red crystals of the product were isolated (50 mg, 29%). M.p. (dec): 167 °C. ^{1}H-NMR ($CDCl_3$): $\delta = 5.78$ (s, 1H, NH), 5.00 (s, 1H, α-C_5H_4), 4.78 (s, 2H, β-C_5H_4), 4.59 (s, 1H, α-C_5H_4), 4.40 (s, 5H, C_5H_5), 4.05 (m, 1H, Cy), 3.04 (m, 1H, Cy), 2.25 (m, 1H, Cy), 2.0–1.0 (m, 19H, Cy).

$^{13}C\{^{1}H\}$-NMR ($CDCl_3$, 75.5 MHz): $\delta = 183.4$ (d, $^{1}J_{Rh-C} = 72.1$ Hz), 182.5 (d, $^{1}J_{Rh-C} = 69.4$ Hz), 180.0 (d, $^{2}J_{Rh-C} = 4.2$ Hz), 75.2, 73.7, 71.9, 69.9, 67.0, 59.6, 58.8, 34.9, 34.3, 33.9, 31.6, 25.1, 25.0, 24.6, 24.6, 24.4, 24.3. IR (cm^{-1}): 3208 (m), 2086 (vs), 2016 (vs), 1611 (s), 1460 (vs, br), 1377 (s), 1280 (m), 1094 (m, br), 844 (w), 825 (w), 740 (w), 611 (w), 490 (w), 473 (w). Anal. Found: C, 46.95; H, 5.05; N, 4.37. Calc. for $C_{25}H_{32}BF_4FeN_2O_2Rh$: C, 47.06; H, 5.05; N, 4.39%.

2.3. X-ray crystallographic studies

Table 1 lists a summary of crystallographic data for all crystallographically characterized compounds. Details of individual data collections and solutions are given below.

2.3.1. General procedure

A crystal of appropriate size was mounted on a quartz fiber using Paratone-N hydrocarbon oil, transferred to a Siemens SMART diffractometer/CCD area detector [16], centered in the beam (Mo–K_α; $\lambda = 0.71073$ Å; graphite monochromator), and cooled by a nitrogen low-temperature apparatus. Preliminary orientation matrix and cell constants were determined by collection of 60 10-s frames, followed by spot integration and least-squares refinement. A hemisphere of data was collected using 0.3°ω scans. The raw data were integrated (XY spot spread = 1.60°, Z spot spread = 0.60°) and the unit cell parameters refined using SAINT. Data analysis and absorption correction was performed using XPREP. The data were corrected for Lorentz and polarization effects, but no correction for crystal decay was applied. The structure was solved and refined with the TEXSAN [17] software package using direct methods and expanded using Fourier techniques. The quantity minimized by the least-squares program was $\Sigma w(|F_o| - |F_c|)^2$, where w is the weight of a given observation. The p-factor, used to reduce the weight of intense reflections, was set to 0.030 throughout the refinement. The

Table 1
Crystal data and collection parameters

Compound	FcC(NCy)NHCy	CpFe(CO)-[FcC(NCy)N(Cy)C(O)]	CpFe(CO)-[FcC(NCy)$_2$]	[FcC(NCy)$_2$]-Rh(CO)$_2$	{[FcC(NCy)NHCy]-Rh(CO)$_2$}[BF_4]
Empirical formula	$C_{23}H_{32}FeN_2$	$C_{30}H_{36}N_2O_2Fe_2$	$C_{29}H_{36}N_2OFe_2$	$C_{25}H_{31}N_2O_2RhFe$	$C_{25}H_{32}BF_4O_2RhFeN_2$
Formula weight	392.37	568.32	540.30	550.29	638.14
Space group	$P2_12_12_1$ (#19)	$P2_12_12_1$ (#19)	$P\bar{1}$ (#2)	$Pba2$ (#32)	$P\bar{1}$ (#2)
Temperature (°C)	−150	−104	−93	−93	−97
Unit cell dimensions					
a (Å)	39.547(1)	9.9667(1)	10.0875(2)	19.0364(5)	10.0949(3)
b (Å)	9.3790(2)	17.9689(4)	11.6278(2)	21.0181(6)	10.9287(3)
c (Å)	10.7050(2)	28.9218(5)	13.0580(1)	5.8973(2)	13.0603(4)
α (°)			83.185(1)		108.915(1)
β (°)			68.016(1)		97.231(1)
γ (°)			64.307(1)		99.928(1)
V (Å^3)	3970.6(1)	5179.6(2)	1278.11(4)	2359.6(2)	1316.9(1)
Z	8	8	2	4	2
Diffractometer	Siemens SMART	Siemens SMART	Siemens SMART	Siemens SMART	Siemens SMART
Radiation	Mo–K_α ($\lambda = 0.71073$ Å)	Mo–K_α ($\lambda = 0.71073$ Å)	Mo–K_α ($\lambda = 0.71073$ Å)	Mo–K_α ($\lambda = 0.71073$ Å)	Mo–K_α ($\lambda = 0.71073$ Å)
Monochromator	Graphite	Graphite	Graphite	Graphite	Graphite
Detector	CCD area detector	CCD area detector	CCD area detector	CCD area detector	CCD area detector
Scan type, width	ω, 0.3°	ω, 0.3°	ω, 0.3°	ω, 0.3°	ω, 0.3°
Scan speed	10 s frame^{-1}	30 s frame^{-1}	20 s frame^{-1}	10 s frame^{-1}	30 s frame^{-1}
Reflections measured	Hemisphere	Hemisphere	Hemisphere	Hemisphere	Hemisphere
2θ Range (°)	3–46.5	3–46.5	3–46.5	3–46.5	3–46.5
μ (mm^{-1})	0.768	1.15	1.16	1.336	1.229
T_{min}, T_{max}	0.622, 0.760	0.822, 0.897	0.797, 0.880	0.773, 0.861	0.853, 0.923
Crystal dimensions (mm)	0.30 × 0.32 × 0.32	0.22 × 0.15 × 0.09	0.22 × 0.20 × 0.11	0.14 × 0.13 × 0.10	0.12 × 0.11 × 0.08
Color	Orange	Orange–red	Red	Orange	Red
Number of reflections measured	16 799	21 373	5255	9966	5529
Number of unique reflections	3283	7426	3561	3539	3681
Number of observations	2685	6145	3110	2533	2923
Number of parameters	475	649	307	279	329
R, R_w (%)	3.10, 3.67	2.67, 3.16	3.47, 4.98	2.55, 3.02	3.96, 5.11
Goodness-of-fit	1.25	1.07	1.92	1.00	1.76

analytical forms of the scattering factor tables for the neutral atoms were used, and all scattering factors were corrected for both the real and imaginary components of anomalous dispersion [18].

2.3.2. FcC(NCy)NHCy

Crystals suitable for X-ray diffraction studies were grown over several days by the slow cooling of a boiling hexanes solution to r.t. Data collection and processing proceeded as stated above.

The unit cell parameters indicated a primitive orthorhombic cell. Systematic absences indicated the space group $P2_12_12_1$ (# 19); this was confirmed by the successful refinement of the model. All non-hydrogen atoms were refined anisotropically. Amine hydrogens were located in a difference Fourier map, and their positions were refined. All remaining hydrogens were assigned idealized positions and were included in structure factor calculations, but were not refined. The Flack parameter was refined to 0.53, indicative of inversion twinning. Friedel mates were averaged.

2.3.3. CpFe(CO)[FcC(NCy)N(Cy)C(O)]

Crystals suitable for X-ray diffraction studies were grown over several days by vapor diffusion of hexanes into an Et_2O solution of the compound. Data collection and processing proceeded as stated above.

The unit cell parameters indicated a primitive orthorhombic cell. Systematic absences indicated the space group $P2_12_12_1$ (# 19); this was confirmed by the successful refinement of the model. All non-hydrogen atoms were refined anisotropically. Hydrogen atoms were assigned idealized positions and were included in structure factor calculations but were not refined. The Flack parameter was refined to 1.006(3), indicating that the incorrect absolute configuration had been used ($R = 3.89\%$, $R_w = 4.74\%$). Atomic coordinates were inverted and the Flack parameter refined to $-0.036(2)$. The final residuals improved significantly ($R = 2.67\%$, $R_w = 3.16\%$).

2.3.4. CpFe(CO)[FcC(NCy)$_2$]

Crystals suitable for X-ray diffraction studies were grown from hexanes at -40 °C. Data collection and processing proceeded as stated above.

The unit cell parameters indicated a triclinic cell. The choice of the centric space group was confirmed by the successful solution of the structure. All non-hydrogen atoms were refined anisotropically. Hydrogen atoms were assigned idealized positions and were included in structure factor calculations but were not refined.

2.3.5. [FcC(NCy)$_2$]Rh(CO)$_2$

Crystals suitable for X-ray diffraction studies were grown from hexanes at 5 °C. Data collection and processing proceeded as stated above.

The unit cell parameters and systematic absences indicated a primitive orthorhombic cell. The choice of the acentric space group $Pba2$ (# 32) was confirmed by successful solution of the structure. All non-hydrogen atoms were refined anisotropically. Hydrogen atoms were assigned idealized positions and were included in structure factor calculations but were not refined. Initial refinement of the incorrect absolute structure (Flack parameter = 0.945(9)) gave residuals of $R = 3.07\%$ and $R_w = 3.63\%$. The atomic coordinates were inverted and the Flack parameter refined to 0.013(8) indicating that the correct absolute structure was used. The final residuals improved significantly ($R = 2.55\%$, $R_w = 3.02\%$).

2.3.6. {[FcC(NCy)NHCy]Rh(CO)$_2$}[BF$_4$]

Crystals suitable for X-ray diffraction studies were grown from CH_2Cl_2–Et_2O at -40 °C. Data collection and processing proceeded as stated above.

The unit cell parameters indicated a primitive triclinic cell. The choice of the centric space group was confirmed by successful solution of the structure. All non-hydrogen atoms were refined anisotropically. The amidine hydrogen was located in a difference Fourier and refined isotropically. All remaining hydrogen atoms were assigned idealized positions and were included in structure factor calculations but were not refined.

3. Results and discussion

3.1. Ligand synthesis and characterization

Deprotonation of ferrocene with one equivalent *t*-BuLi in THF–hexanes forms a mixture of ferrocenyl lithium (FcLi), the 1,1′-dilithio species ($FcLi_2$), and unreacted ferrocene [19]. This mixture reacts readily with DCC to generate amidinate products, with FcC(NCy)$_2$Li being the major species formed. It is noteworthy that an attempt to prepare the *N*,*N*′-bis(trimethylsilyl) analogue by similar methodology has been reported to give no reaction [1a], apparently due to the lower electrophilicity of the trimethylsilyl-substituted carbodiimide. In order to isolate pure ligand, the mixture was hydrolyzed with excess water, and the solvent was stripped to afford an orange mixture consisting of FcC(NCy)NHCy, Fc[C(NCy)NHCy]$_2$ [20], and Cp_2Fe (Scheme 1).

Sublimation of the mixture at 65 °C/10^{-2} mmHg removed ferrocene and carbodiimide; pure FcC(NCy)NHCy was then obtained in 50% yield by crystallization of the residue from boiling hexanes.

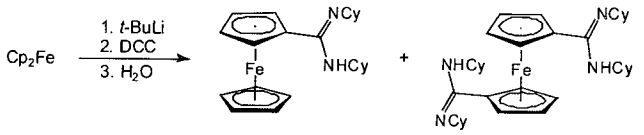

Scheme 1.

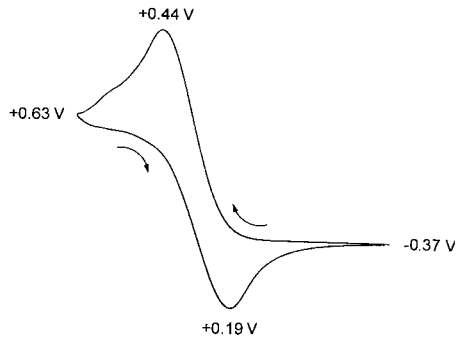

Fig. 1. Cyclic voltammogram of a 10^{-2} M solution of FcC(NCy)NHCy in CH_2Cl_2 measured at 50 mV s^{-1} (referenced to Cp_2Fe couple).

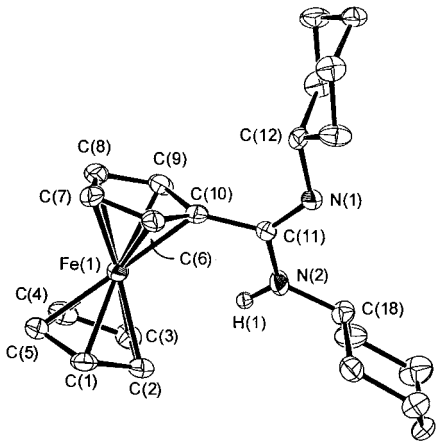

Fig. 2. ORTEP view of one of the two independent molecules of FcC(NCy)NHCy drawn with 50% thermal ellipsoids.

Table 2
Selected bond lengths (Å) and bond angles (°) for FcC(NCy)NHCy

Fe1–C1	2.072(5)	Fe1–C2	2.074(5)
Fe1–C3	2.042(5)	Fe1–C4	2.053(5)
Fe1–C5	2.054(5)	Fe1–C6	2.057(5)
Fe1–C7	2.042(5)	Fe1–C8	2.051(5)
Fe1–C9	2.052(5)	Fe1–C10	2.072(5)
N1–C11	1.289(6)	N2–C11	1.370(6)
N2–H1	0.88(6)		
C11–N1–C12	120.8(4)	C11–N2–C18	125.0(4)
C11–N2–H1	114(3)	C18–N2–H1	121(3)
N1–C11–N2	121.5(4)	N1–C11–C10	126.0(4)
N2–C11–C10	112.3(4)		

Infrared spectroscopy of air-stable FcC(NCy)NHCy reveals absorbances at 1619 and 3420 cm^{-1} which are assigned to $\nu_{C=N}$ and ν_{N-H}, respectively. ^{1}H-NMR spectroscopic data of C_6D_6 solutions show a single species with two distinct triplets of equal intensities at 4.28 and 3.93 ppm arising from the substituted-Cp ligand and a singlet at 3.99 ppm from the other Cp ligand. Cyclic voltammetry reveals a quasi-reversible oxidation at $E_{1/2} = +0.31$ V relative to the $Cp_2Fe/[Cp_2Fe]^+$ couple (Fig. 1). The ΔE_p of 250 mV is only slightly greater than that measured for Cp_2Fe (220 mV) under analogous conditions. The solid-state structure was determined by X-ray crystallography. A drawing of one of the two independent molecules (per asymmetric unit) is shown in Fig. 2 with related metrical parameters in Table 2. Since the two molecules are essentially structurally identical, only one will be discussed. As expected, the amidine functionality displays localized single and double CN bonds of 1.467(6) and 1.289(6) Å for N(2)–C(11) and N(1)–C(11), respectively. Due to the high quality of the data set, the amidine-hydrogen bound to N(2) was located in a difference Fourier map, and it was refined isotropically. The N(1)–C(11)–N(2)–C(18) torsion angle is only 8.6(9)°, and the geometry at N(2) is planar (combined angles = 360°). These data suggest π-delocalization over N(1)–C(11)–N(2) similar to that found in organic amides. The substituted-Cp plane is roughly perpendicular to the NCN group, intersecting at 71°.

3.2. Synthesis and characterization of Group 1 and transition metal derivatives

The free-base FcC(NCy)NHCy was easily converted to the lithium salt by deprotonation with $LiN(SiMe_3)_2$ in toluene. Concentration of the solution followed by the addition of Et_2O resulted in crystallization of the etherate, $\{[FcC(NCy)_2]Li(Et_2O)\}_2$, in 90% yield. The sodium derivative was prepared similarly using $NaN(SiMe_3)_2$, however, the product was isolated as an orange powder from hexanes.

Similar to other lithium amidinates, $\{[FcC(NCy)_2]Li(Et_2O)\}_2$ functions as a useful reagent in salt-metathesis reactions with metal halides. For example, treatment of $FeCl_2$ with two equivalents of $[FcC(NCy)_2]Li(Et_2O)$ in THF, followed by crystallization from CH_2Cl_2–Et_2O, afforded orange crystals of the trimetallic $[FcC(NCy)_2]_2Fe$ in good yield (Scheme 2). A similar reaction with $CoBr_2$ in Et_2O gave $[FcC(NCy)_2]_2Co$, also in good yield. We note that these compounds are rare examples of monomeric homoleptic amidinates of Fe(II) and Co(II) [6e]. We attribute their stability to the relatively high degree of steric protection provided by the cyclohexyl groups. Magnetic susceptibility measurements (by Evans' solution NMR method) gave μ_{eff} values typical for high spin Fe(II) and Co(II) (5.02 and 4.62 μ_B, respectively). In an attempt to prepare a mixed cyclopentadienyl-amidinate derivative, $CpFe(CO)_2I$ was

reacted with $[FcC(NCy)_2]Li(Et_2O)$ in toluene. The initially black solution became orange–brown within a few minutes indicating the absence of any $CpFe(CO)_2I$.

The isolation of pure product, however, proved to be difficult due to the moderate solubility of the byproduct LiI. This problem was remedied by the use of the ether-free sodium salt $[FcC(NCy)_2]Na$. Stirring the reactants in toluene overnight afforded an orange–red

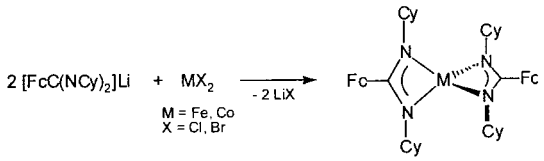

Scheme 2.

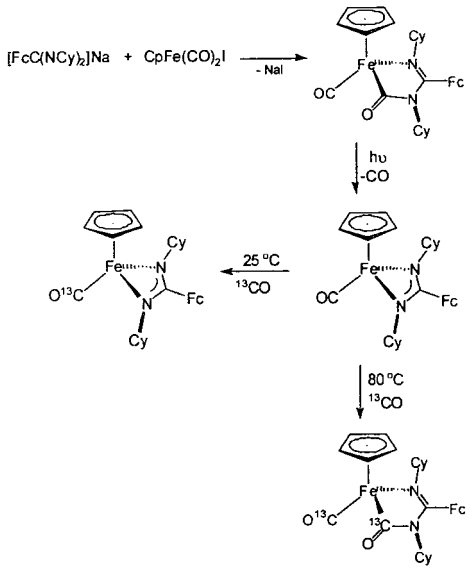

Scheme 3.

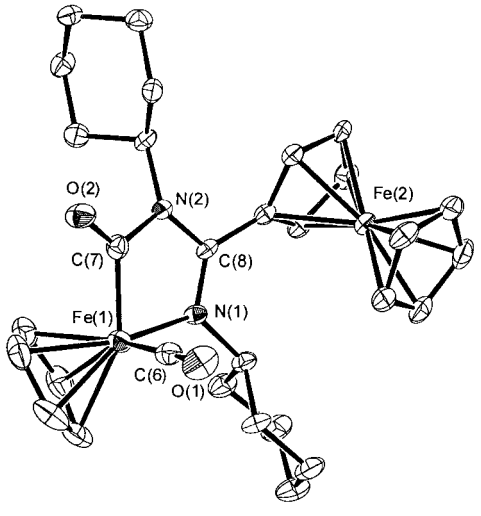

Fig. 3. ORTEP view of CpFe(CO)[FcC(NCy)N(Cy)C(O)] drawn with 50% thermal ellipsoids.

Table 3
Selected bond lengths (Å) and bond angles (°) for CpFe(CO)-[FcC(NCy)N(Cy)C(O)]

Fe(1)–N(1)	1.975(3)	Fe(1)–C(1–5)$_{ave}$	2.119
Fe(1)–C(6)	1.731(4)	Fe(1)–C(7)	1.904(4)
O(1)–C(6)	1.163(4)	O(2)–C(7)	1.223(4)
N(1)–C(8)	1.315(4)	N(2)–C(7)	1.442(5)
N(2)–C(8)	1.380(4)		
N(1)–Fe(1)–C(6)	92.9(2)	N(1)–Fe(1)–C(7)	81.8(1)
C(6)–Fe(1)–C(7)	90.3(2)	Fe(1)–N(1)–C(8)	114.8(2)
C(7)–N(2)–C(8)	113.5(3)	Fe(1)–C(6)–O(1)	178.1(4)
Fe(1)–C(7)–O(2)	129.0(3)	Fe(1)–C(7)–O(2)	129.0(3)
Fe(1)–C(7)–N(2)	112.8(3)	O(2)–C(7)–N(2)	118.0(3)
N(1)–C(8)–N(2)	115.7(3)		

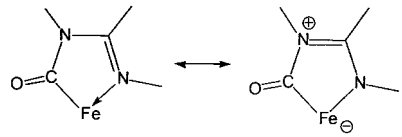

Scheme 4.

solution and yellow precipitate. Work-up in toluene–hexanes followed by cooling to -40 °C afforded pure CpFe(CO)[FcC(NCy)N(Cy)C(O)] as microcrystalline orange–red solid in good yield (Scheme 3).

Despite reports of a closely related reaction ($CpFe(CO)_2Cl + Li$(amidinate)) yielding an unstable product [1b], our product proved to be air-stable in Et_2O solution, as well as thermally stable in boiling benzene. Characterization by IR spectroscopy revealed an intense absorption at 1902 cm^{-1} assignable to the terminal ν_{CO} and additional absorptions at 1630 and 1514 cm^{-1} for C=O and C=N stretches of the carbamoyl-type ligand. For comparison, the related Mn complex $Mn(CO)_4$[PhC(NPh)N(Ph)C(O)] features an absorption at 1673 cm^{-1} assigned to $\nu_{C=O}$ [21]. $^{13}C\{^1H\}$-NMR spectroscopic data also support the formulation of the product with downfield signals at δ 223.8 and 220.3 ppm for the carbonyl carbons (absolute assignments are not made). The structure was further confirmed by X-ray crystallography. A drawing of one of the two independent molecules per asymmetric unit is shown in Fig. 3 with corresponding metrical parameters in Table 3. The N(l)–C(8) distance of 1.315(4) Å is longer than expected for a double bond, and the N(2)–C(8) interaction of 1.380(4) Å is shorter than expected for a single bond (compare to N(2)–C(7), 1.442(5) Å). This suggests significant contribution from the zwitterionic resonance form shown in Scheme 4. Additionally, the geometry at N(2) is nearly planar with the sum of the angles equaling 357.5°.

The carbonyl ligand of CpFe(CO)[FcC(NCy)-N(Cy)C(O)] was found to be thermally inert. Heating C_6D_6 solutions of the complex in the presence of ^{13}CO (14 psig) to 85 °C overnight failed to incorporate any

labeled CO into the Fe complex. Likewise, heating a benzene solution to reflux under N_2 overnight failed to give any reaction. Photolysis, however, led to the loss of CO and the formation of air-sensitive CpFe(CO)-[FcC(NCy)$_2$] (Scheme 3). For convenience, the reaction can be carried out using a solution of CpFe(CO)[FcC-(NCy)N(Cy)C(O)] generated in situ from CpFe(CO)$_2$I and [FcC(NCy)$_2$]Na. Following this preparation, the dark red product was readily isolated in 27% yield. IR spectroscopic data shows a strong absorption at 1929 cm^{-1} assigned as ν_{CO}, which is blue-shifted relative to the related parameter of CpFe(CO)[FcC(NCy)-N(Cy)C(O)] ($\nu_{CO} = 1902$ cm^{-1}). Characterization by $^{13}C\{^1H\}$-NMR spectroscopy reveals a signal at δ 223.2 ppm for the carbonyl ligand. The solid-state structure, as determined by X-ray crystallography, was consistent with the spectroscopic data. An ORTEP view of the molecule is shown in Fig. 4 with related bond lengths and angles in Table 4. As expected, the Fe–N bonds of the amidinate ligand are nearly identical at 1.995(3) and 2.009(2) Å. The carbonyl ligand is typical, with an Fe–C(1) distance of 1.738(3) Å and an Fe–C(1)–O(1) angle of 177.0(3)°.

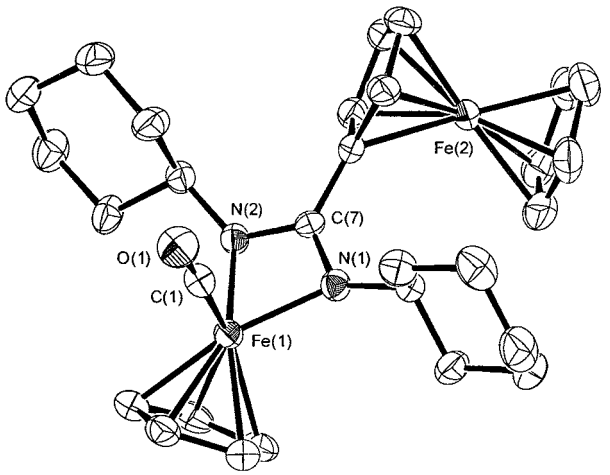

Fig. 4. ORTEP view of CpFe(CO)[FcC(NCy)$_2$] drawn with 50% thermal ellipsoids.

Table 4
Selected bond lengths (Å) and bond angles (°) for CpFe(CO)-[FcC(NCy)$_2$]

Fe(1)–N(1)	1.995(3)	Fe(1)–N(2)	2.009(2)
Fe(1)–C(1)	1.738(3)	Fe(1)–C(2–6)$_{ave}$	2.104
O(1)–C(1)	1.165(4)	N(1)–C(7)	1.326(4)
N(2)–C(7)	1.337(4)		
N(1)–Fe(1)–N(2)	65.4(1)	N(1)–Fe(1)–C(1)	95.9(1)
N(2)–Fe(1)–C(1)	95.8(1)	Fe(1)–N(1)–C(7)	93.1(2)
Fe(1)–N(2)–C(7)	92.1(2)	Fe(1)–C(1)–O(1)	177.0(3)

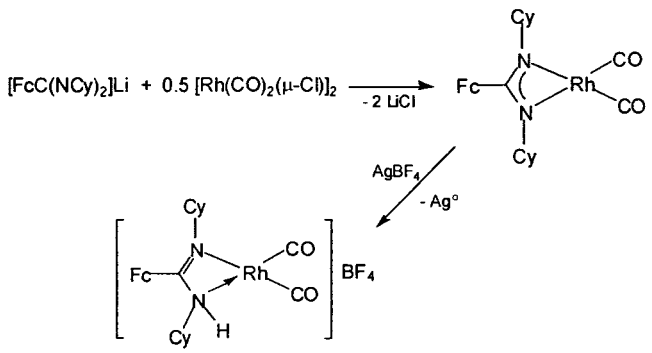

Scheme 5.

In contrast to the carbarmoyl-type derivative, the carbonyl ligand of CpFe(CO)[FcC(NCy)$_2$] readily exchanges with ^{13}CO (50 psig) in C_6D_6 solution at 25 °C (Scheme 3). The reaction likely proceeds via the 16-electron intermediate CpFe[FcC(NCy)$_2$], formed by disassociative loss of CO, although an η^1-amidinate ligand cannot be ruled out. When the same solution was heated to 80 °C for 7 h, 65% conversion to the doubly labeled carbamoyl derivative was observed.

We anticipated that oxidizing the ferrocenyl group of FcC(NCy)$_2$ might alter the donor properties of the ligand. In order to probe the effect of this oxidation, we sought to prepare a metal carbonyl derivative that would be preferentially oxidized at the Fc site. This would allow us to monitor the ν_{CO} (by IR spectroscopy) as a function of ligand oxidation state. The molecule we prepared for this purpose is [FcC(NCy)$_2$]Rh(CO)$_2$. As shown in Scheme 5, the lithium salt readily reacted with [Rh(CO)$_2$(μ-Cl)]$_2$ in toluene to form the desired product in good yield.

IR spectroscopy revealed two intense absorptions at 2052 and 1977 cm^{-1} assigned to the terminal carbonyls. $^{13}C\{^1H\}$-NMR spectroscopic data, which showed a doublet at δ 182.3 ppm ($^2J_{Rh-C} = 4.4$ Hz) for the amidine (NCN) carbon, suggested that the complex was monomeric in solution. X-ray crystallography proved this to be the case in the solid-state as well.

Shown in Fig. 5 is an ORTEP diagram with related bond angles and lengths in Table 5. The square-planar rhodium features an η^2-amidinate ligand and a pair of terminal carbonyls. The Rh–N bonds are essentially identical (avg. 2.066 Å) as are the Rh–C bonds (avg. 1.857 Å). The substituted-Cp plane intersects the NCN plane at a dihedral angle of 47°.

As shown in Fig. 6, cyclic voltammetry measurements of [FcC(NCy)$_2$]Rh(CO)$_2$ (taken at 200 mV s^{-1}) reveal a quasi-reversible oxidation of the Fc-group at $E_{1/2} = +0.46$ V (vs. Cp$_2$Fe) with an additional irreversible oxidation at +1.49 V. Chemical oxidation of [FcC(NCy)]Rh(CO)$_2$ with 1 equivalent of AgBF$_4$ in CH_2Cl_2 appeared to occur quickly, with a silver precipitate forming within minutes. Following methylene chloride work-up, the product was isolated as red crystals from CH_2Cl_2–Et_2O in 29% yield. IR spectroscopy revealed an absorption at 3208 cm^{-1}, which appeared to be due a N–H stretch and a strong absorption at

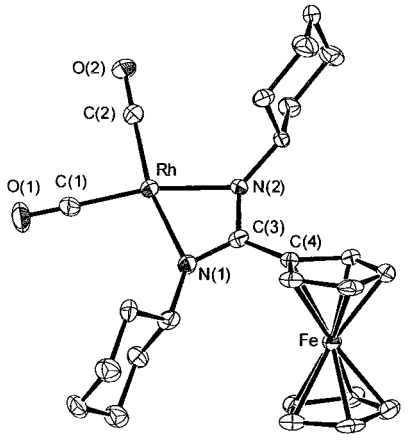

Fig. 5. ORTEP view of $[FcC(NCy)_2]Rh(CO)_2$ drawn with 50% thermal ellipsoids.

Table 5
Selected bond lengths (Å) and bond angles (°) for $[FcC(NCy)_2]Rh(CO)_2$

Rh–N1	2.062(4)	Rh–N2	2.069(4)
Rh–C1	1.861(6)	Rh–C2	1.852(6)
O1–C1	1.132(6)	O2–C2	1.142(6)
N1–C3	1.324(7)	N2–C3	1.343(6)
C3–C4	1.487(7)		
N1–Rh–N2	63.8(2)	N1–Rh–C1	104.0(2)
N1 –Rh–C2	166.3(2)	N2–Rh–C1	167.8(2)
N2–Rh–C2	102.4(2)	C1–Rh–C2	89.7(2)
Rh–C1–O1	178.9(6)	Rh–C2–O2	178.4(5)

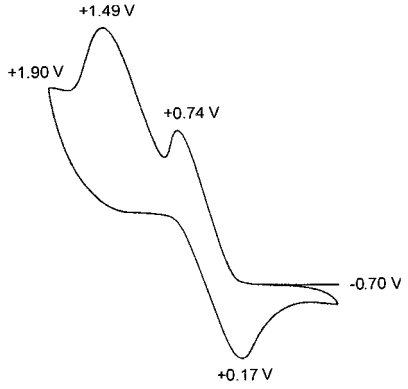

Fig. 6. Cyclic voltammogram of a 10^{-2} M solution of $[FcC(NCy)_2]Ph(CO)_2$ in THF measured at 200 mV s^{-1} (referenced to Cp_2Fe couple).

1611 cm^{-1}, likely from a CN double bond. Additionally, the ^{1}H-NMR spectrum contained a singlet at 5.78 ppm that integrated to a single hydrogen, further suggesting the formation of an amidine functionality. As shown in Fig. 7, X-ray crystallography revealed the product to be $\{[FcC(NCy)NHCy]Rh(CO)_2\}[BF_4]$, which contains ferrous Fc-group and a coordinated η^2-amidine. Similar to $[FcC(NCy)_2]Rh(CO)_2$, the 4-coordinate rhodium adopts square-planar geometry. As expected, the Rh–N(1) bond (2.063(5) Å) is shorter than the dative Rh–N(2) bond (2.131(5) Å). This results in a *trans* influence that is observed as a slight elongation of the Rh–C(2) bond (1.864(7) Å) compared to Rh–C(1) (1.846(7) Å) (Table 6). Interestingly, unlike all of the structurally characterize, Fc-containing amidinates, the substituted-Cp plane is nearly coplanar with the NCN amidine plane (dihedral angle = 7°). It appears likely that this is simply caused by steric repulsions; the cyclohexyl group bound to N(2) is directed away from the Cp-hydrogens.

In conclusion, we have reported a convenient large-scale synthesis of the ferrocene-containing amidinate ligand $FcC(NCy)_2$. This ligand can be used for the stabilization of a wide range of transition metal derivatives which feature good solubility and crystallization properties. Although electrochemical studies suggest that oxidation of the ferrocenyl moiety is possible, the isolation of ferrocenium-containing derivatives has proven to be difficult. Further study of the redox properties will be necessary for the development of redox-switchable ligands.

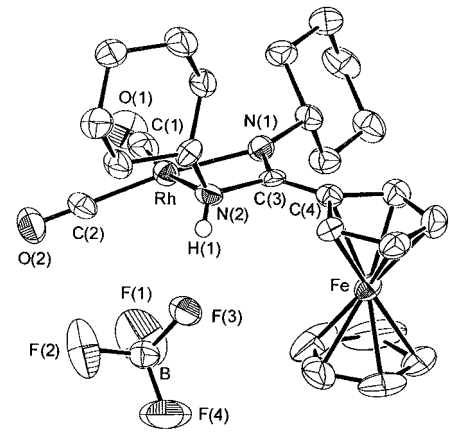

Fig. 7. ORTEP view of $\{[FcC(NCy)NHCy]Rh(CO)_2\}[BF_4]$ drawn with 50% thermal ellipsoids.

Table 6
Selected bond lengths (Å) and bond angles (°) for $\{[FcC(NCy)NHCy]Rh(CO)_2\}[BF_4]$

Rh–N1	2.063(5)	Rh–N2	2.131(5)
Rh–C1	1.846(7)	Rh–C2	1.864(6)
O1–C1	1.149(8)	O2–C2	1.136(7)
N1–C3	1.279(7)	N2–C3	1.481(7)
C3–C4	1.436(8)		
N1–Rh–N2	63.6(2)	N1–Rh–C1	105.6(2)
N1–Rh–C2	167.2(2)	N2–Rh–C 1	169.0(2)
N2–Rh–C2	103.8(2)	C1–Rh–C2	87.1(3)
Rh–C1–O1	178.0(6)	Rh–C2–O2	179.4(6)

4. Supplementary material

Crystallographic data for the structural analysis have been deposited with the Cambridge Crystallographic Data Centre, CCDC nos. 157181–157185. Copies of this information may be obtained free of charge from The Director, CCDC, 12 Union Road, Cambridge CB2 1EZ, UK (Fax: +44-1223-336033; e-mail: deposit@ccdc.cam.ac.uk or www: http://www.ccdc.cam.ac.uk).

Acknowledgements

We thank the DOE (contract no. DE-AC03-76SF00098) for support of this work.

References

[1] (a) F.T. Edelmann, Coord. Chem. Rev. 137 (1994) 403;
(b) J. Barker, M. Kilner, Coord. Chem. Rev. 133 (1994) 219;
(c) K. Dehnicke, Chem.-Ztg. 114 (1990) 295.

[2] (a) P. Berno, S. Hao, R. Minhas, S. Gambarotta, J. Am. Chem. Soc. 116 (1994) 7417;
(b) F.A. Cotton, L.M. Daniels, C.A. Murillo, X. Wang, J. Am. Chem. Soc. 118 (1996) 4830.

[3] J.R. Hagadorn, J. Arnold, Organometallics 17 (1998) 1355.

[4] (a) K. Shibayama, S.W. Seidel, B.M. Novak, Macromolecules 30 (1997) 3159;
(b) S.R. Foley, Y. Zhou, G.P.A. Yap, D.S. Richeson, Inorg. Chem. 39 (2000) 924;
(c) R. Duchateau, C.T. van Wee, J.H. Teuben, Organometallics 15 (1996) 2291.

[5] (a) J.M. Decker, S.J. Geib, T. Meyer, Organometallics 18 (1999) 4417;
(b) M.P. Coles, R.F. Jordan, J. Am. Chem. Soc. 119 (1997) 8125;
(c) C. Averbuj, E. Tish, M.S. Eisen, J. Am. Chem. Soc. 120 (1998) 8640;
(d) J.C. Florez, J.C.W. Chien, M.D. Rausch, Organometallics 14 (1995) 1827;
(e) R. Gomez, R. Duchateau, A.N. Chernega, A. Meetsma, F.T. Edelmarm, J.H. Teuben, M.L.H. Green, J. Chem. Soc. Dalton Trans. (1995) 217.

[6] (a) J.A.R. Schmidt, J. Arnold, Chem. Commun. (1999) 2149;
(b) P.J. Stewart, A.J. Blake, P. Mountford, Organometallics 17 (1998) 3271–3281;
(c) Y. Zhou, D.S. Richeson, Inorg. Chem. 35 (1996) 2448;
(d) A. Littke, N. Sleiman, C. Bensimon, D.S. Richeson, G.P.A. Yap, S.J. Brown, Organometallics 17 (1998) 446;
(e) B. Vendemiati, G. Prini, A. Meetsma, B. Hessen, J.H. Teuben, O. Traverso, Eur. J. Inorg. Chem. 3 (2001) 707–711.

[7] (a) J.R. Hagadorn, J. Arnold, Angew. Chem. Int. Ed. Engl. 37 (1998) 1729;
(b) G.D. Whitener, J.R. Hagadorn, J. Arnold, J. Chem. Soc. Dalton Trans. (1999) 1249.

[8] (a) K. Kiincaid, C.P. Gerlach, G.R. Giesbrecht, J.R. Hagadorn, G.D. Whitener, A. Shafir, J. Arnold, Organometallics 18 (1999) 5360;
(b) M.J.R. Brandsma, E.A.C. Brussee, A. Meetsma, B. Hessen, J.H. Teuben, Eur. J. Inorg. Chem. (1998) 1867.

[9] For a recent review of this general area, see the following and references therein: A.M. Allgeier, C.A. Mirkin, Angew. Chem. Int. Ed. Engl. 37 (1998) 894.

[10] E.H. Amonoo-Neizer, R.A. Shaw, D.O. Skovlin, B.C. Smith, Inorg. Synth. 8 (1966) 19.

[11] C.R. Krüger, H. Niederprüm, Inorg. Synth. 8 (1966) 15.

[12] (a) J.A. McCleverty, G. Wilkinson, Inorg. Synth. 8 (1966) 211;
(b) R. Cramer, Inorg. Synth. 15 (1974) 17.

[13] R.B. King, F.G.A. Stone, Inorg. Synth. 7 (1963) 110.

[14] W.A. Hermann, C. Zybill, in: W.A. Hermann, A. Slazer (Eds.), Synthetic Methods of Organometallic and Inorganic Chemistry, vol. 1, Thieme, New York, 1996, p. 81.

[15] (a) D.F. Evans, J. Chem. Soc. (1959) 2003;
(b) E.M.J. Schubert, J. Chem. Educ. 69 (1992) 62.

[16] SMART Area-Detector Software Package, Siemens Industrial Automation, Inc., Madison, WI, 1993.

[17] TEXSAN: Crystal Structure Analysis Package, Molecular Structure Corporation, 1992.

[18] $R = [\Sigma \| F_o| - |F_c \|]/\Sigma |F_o|$, $R_w = \{[\Sigma_w(|F_o| - |F_c|)^2]/\Sigma_w F_o^2\}^{1/2}$, goodness-of-fit $= \{[\Sigma_w(|F_o| - |F_c|)^2]/(n_o - n_v)\}^{1/2}$, where n_o is the number of observations, n_v is the number of variable parameters, and the weights w were given by: $w = 1/\sigma_2(F_o)$, $\sigma(F_o^2) = [\sigma_o^2(F_o^2) + (pF_o^2)^2]^{1/2}$, where $\sigma^2(F_o)$ is calculated as above from $\sigma(F_o)^2$ and where p is the factor used to lower the weight of intense reflections.

[19] D. Guillaneux, H.B. Kagan, J. Org. Chem. 60 (1995) 2503.

[20] J.R. Hagadorn, J. Arnold, unpublished results.

[21] T. Inglis, M. Kilner, T. Reynoldson, E.E. Robertson, J. Chem. Soc. Dalton Trans. (1975) 924.